



# Magnetic field sensor based on nickel-coated S-shaped long period fiber grating

Chao-Wei Wu<sup>1</sup>

Received: 26 April 2018 / Accepted: 11 September 2018 / Published online: 18 September 2018  
© Springer Science+Business Media, LLC, part of Springer Nature 2018

## Abstract

The paper presents the fabrication of S-shaped metallic long period fibre grating (MLPFG) based on electroforming process for the realization of metal-based micro-electro-mechanical systems magnetic field sensors. The fabricated S-shaped MLPFG sensors were then tested in a magnetic field experiment. The NdFeB magnet was used to control the size of the magnetic field, and a gaussmeter was used to measure the magnetic field to analyse the spectral changes in the sensor in different magnetic fields. The results showed that an external magnetic load (NdFeB magnet) attracted the nickel structure, which changed the periodic metal structure size, disturbing the refractive index of the LPFG structure and altering the coupling coefficient, which increased the transmission loss as the magnetic field varied from 0 to 350 Gauss. The optimal sensitivity of the magnetic field to the loss was  $-0.0084$  dB/Gauss and  $R^2$  was 0.9426. Therefore, the S-shaped metallic LPFG sensor developed in this study can be used to detect magnetic fields.

**Keywords** Magnetic field sensor · Electroforming process · MEMS process · Long period fibre grating

## 1 Introduction

In recent years, optical fibre sensors have been widely used in engineering applications to monitor different physical and chemical parameters such as magnetic field (Yang et al. 2009; Thomas et al. 2010; Zheng et al. 2013; Liu et al. 2014), temperature (Singh et al. 2014; Najari et al. 2015; Lv et al. 2018), strain (Zheng et al. 2018; Del Villar et al. 2018), humidity (Berruti et al. 2014; Jiao et al. 2017), pH (Mishra et al. 2017; Zhao et al. 2018), biomedical parameters (Bandara et al. 2015; Yin et al. 2016), and refractive index (RI)

---

This article is part of the Topical Collection on Optics in Materials, Energy and Related Technologies 2018.

---

Guest Edited by Yen-Hsun Su, Songnan Qu, Yiting Yu, Wei Zhang.

---

✉ Chao-Wei Wu  
cafa95011@gmail.com

<sup>1</sup> Department of Aeronautical and Mechanical Engineering, R.O.C. Air Force Academy, No Sisou 1, Jieshou W. Rd Gangshan Dist, Kaohsiung City 82047, Taiwan, ROC

(Tan et al. 2014; Mizuno et al. 2016; Allsop et al. 2016). Magnetic field sensing is especially important for engineering applications. Optical fibre sensors are more applicable to magnetic field sensing than other types of sensors due to their small size and capacity for use in special circumstances. This paper discusses our survey of past long period fibre grating (LPFG) magnetic field sensor research. Previous studies in this area have utilized LPFG sensors for magnetic field measurements by monitoring their optical spectra. In 2007, Liu et al. (2007) proposed a tunable filter based on LPFG coated with magnetic fluid (MF) as the ambient media. The magnetic sensing spectrum wavelength range of the spectrum measurement is 1510–1555 nm. When the external magnetic field was increased from 0 to 1661 Oe, the wavelength was shifted to the long wavelength by about 7.4 nm. When the MF was subjected to external magnetic fields perpendicularly, the filter's sensitivity in terms of the centre resonant wavelength shift was reported to be 4.455 pm/Oe, and the dip transmission loss was 0.0382 dB/mT. Thomas et al. (2010) reported a long period fibre grating magnetic field sensor with a period of 575  $\mu\text{m}$  based on amorphous magnetic thin films. They used the magnetostrictive characteristics of metallic glass alloys as a mechanism for magnetic field sensing. The saturation magnetostriction of the resulting magnetostrictive sensor was about 1200 gauss, and the resonant wavelength shift was 0.2 nm. The sensitivity of the wavelength to the change of the magnetic field was 0.294 pm/gauss. In 2011, Konstantaki et al. (2011) reported the magnetic tuning of LPFG through the utilization of water- and hydrocarbon-based ferrofluids acting as a cladding layer. When a static magnetic field is perpendicularly applied to this LPFG system, magneto-optical refractive index changes occur in the ferrofluidic cladding. The sensitivity of the system was 0.00125 dB/Gauss. In 2012, Gao et al. (2012) reported a highly sensitive magnetic sensor utilizing D-shaped LPFG immersed into magnetic fluid within a capillary tube. The reason for using the D-shaped fibre was to make the fibre core closer to the external environment for sensing purposes, thus enhancing the sensitivity of the refractive index change itself and, in turn, the sensitivity of the sensor's magnetic field sensing capability. The transmission spectrum results showed that as the intensity of the magnetic field was increased from 1.4 to 191.2 mT, the D-shaped LPFG resonance wavelengths were red-shifted. When the external magnetic field was 189.7 mT, the wavelength shift was 33.46 nm, and the sensitivity of the sensor was 176.4 pm/mT.

In 2013, Miao et al. (2013) proposed a microstructured optical fibre long-period grating magnetic field sensor fabricated by CO<sub>2</sub> laser. The ferrofluid was injected into the microstructures inside the fibre via the capillary effect. Then the two ends of the microstructure fibre were fused by single-mode fibre. The ferrofluid was used as the magnetic field sensing layer, and a magnetic field was used to change the refractive index of the ferrofluid to cause wavelength shift. The results show that the magnetic field measurement range was 0 to 1661 Oe. When the magnetic field was from 0 to 300 Oe, the resonance wavelength shift was more significant and linear, and the sensitivity was 1.946 nm/Oe. When the magnetic field was continuously increased from 300 to 1661 Oe, the wavelength shift was slower. In 2015, Zhang et al. (2015) proposed an LPFG magnetic field sensor fabricated by an ultraviolet radiation processing method to write a periodic structure on single-mode fibre. In addition, a magnetic fluid was used as a magnetic field sensing layer. When an external magnetic field was applied, the magnetic fluid caused the refractive index to be altered, with the index being increased as the intensity of the external magnetic field was increased. When the sensor was immersed in the magnetic fluid, the resonance wavelength was shifted from 1590.8 nm to 1582.9 nm, and the transmission loss was reduced by about 12.5 dB. When the magnetic field was increased from 0 to 108.8 gauss, the resonance wavelength shifted from 1583 nm to 1580 nm, and the transmission loss was reduced by about 19 dB.

Furthermore, the magnetic field sensor could detect a minimum magnetic field of 7.4 Gauss, and the sensor sensitivity was 0.154 dB/gauss. Miao et al. (2015) proposed a tilted LPFG (TLPPFG)-based magnetic sensor with magnetic fluid that was fabricated using CO<sub>2</sub> laser processing. First, a periodic structure with a period of 650 μm and a 70° tilted angle was written on a single-mode fibre to produce the TLPPFG. Next, a magnetic fluid based on Fe<sub>3</sub>O<sub>4</sub> was packaged in the capillaries of the TLPPFG to form a sensing layer that could sense external magnetic field changes. The resulting TLPPFG sensor was characterized by four transmission loss peaks. The sensitivity of the TLPPFG was 0.05 dB/Oe. Gouveia et al. (2017) proposed a long period fibre grating coated with a thin film of nitrogen-doped zinc oxide. The N doping of ZnO increased the magneto-optic properties of the material, which in the presence of the magnetic field changes its own refractive index. The proposed LPFG magnetic field sensor had a period of 650 μm. The result showed linear response with a sensitivity of 2.9 nm/mT in a range of magnetic field between 0 and 10 mT.

These studies utilized the optical fibre sensor for magnetic field measurement by using magnetic fluid, the magneto-optic effect, and the magnetostriction effect. According to the literature, the long-period fibre gratings were fabricated by laser processing. The sensor was demodulated by magnetostrictive effect that used metal film coated with the fibre grating or by the use of a magnetic field to change the refractive index of magnetic fluid, which causes the wavelength and transmission loss changes of the fibre grating sensor. These methods cannot be used in mass production, and the stability of the optical fibre magnetic sensor that utilizes magnetic fluid is questionable. Moreover, few studies thus far have mentioned the possibility of using optical fibre sandwiched in periodic nickel magnetostriction coating for magnetic field measurement. In this study, we propose S-shaped MLPFG magnetic sensors with a S-shaped metallic structure fabricated by electroforming technology. Because of the magnetostriction and magnetic field strain effect of the metallic structure, differing resonant attenuation spectra can be obtained from the S-shaped MLPFG by applying various magnetic fields. Hence, we propose that these periodic S-shaped MLPFG magnetic sensors have the potential for use in compact applications as all-fibre magnetic field sensors.

## 2 Working principle of the S-shaped MLPFG magnetic field sensor

LPFG consists of periodic refractive index variations with periods of 100–000 μm. LPFG promotes coupling between propagating core modes and propagating cladding modes to provide a transmission loss for sensing applications. The proposed S-shaped MLPFG was made of optical fibre sandwiched with a periodic S-shaped polymer-metal (SU-8 photoresist and nickel) structure.

According to the magnetic field of the nickel and the strain-optic effect (Erdogan 1997), when the external magnetic field is applied on the S-shaped MLPFG, the periodic S-shaped nickel and photoresist structure on the optical fibre will induce an expansion strain field in the longitudinal direction of the MLPFG, and the refractive index of the MLPFG will be modulated as a square wave. Based on the strain-optic effect, the refractive indices change linearly in proportion with the strain field.

Hence, the refractive index of the S-shaped MLPFG will be modulated as a periodic square wave distribution along the optical fibre. The transmittance of an S-shaped MLPFG can be expressed with the AC component of the coupling coefficient ( $K_{co-cl}^{ac}$ ) between the

core and the cladding. The transmittance of an S-shaped MLPFG has a cosine-squared relationship and is defined as follows (Erdogan 1997; Shew et al. 2005; Lin et al. 2001):

$$T = \cos^2(\kappa_{co-cl}^{ac} L) \quad (1)$$

where  $L$  indicates the length of the LPFG and  $\kappa_{co-cl}^{ac}$  is the AC component of the coupling coefficient between the core and the cladding. The transmission loss of an MLPFG can be deduced from the AC component of the coupling coefficient between the core and the cladding. Transmission loss is a function of  $\kappa_{co-cl}^{ac}$ , which is proportional to the amplitude of changes in the refractive index because of variation in the strain field.

By using this formula, it can be determined that the transmission loss of an LPFG is a cosine-squared function and that the transmission loss and the resonant wavelength are related to the coupling coefficient and grating length. Therefore, the transmittance can be tuned by changing the external magnetic field. The sensing principle of the S-shaped MLPFG magnetic sensor is thus based on monitoring the transmittance of the S-shaped MLPFG modulated by the magnetic field, where the induced magnetic field strain effect on the S-shaped MLPFG causes changes in the resonant attenuation dip in the S-shaped MLPFG. Our study employed this principle to analyse the characteristics of the magnetic sensor. According to Eq. (1), we can measure the magnetic field by monitoring the transmission loss of the S-shaped MLPFG.

### 3 Process and experimental setup

#### 3.1 The manufacturing of the S-shaped MLPFG magnetic field sensor

The fabrication of the S-shaped MLPFG used in this study was mainly divided into two stages. The first consisted of the lithography process illustrated in Fig. 1, the purpose of which was to produce S-shaped LPFG. The second stage consisted of the electroforming process illustrated in Fig. 2. The LPFG was electroformed to fabricate an LPFG sensor with a nickel metal structure and an S-shaped photoresist structure.

The materials used in the lithography process were SU-8 3050 negative photoresist and etched single mode optical fibre. A 4-inch wafer was sputtered with a copper film approximately 200 nm thick, and the single mode optical fibre was etched to 42  $\mu\text{m}$ -diameter

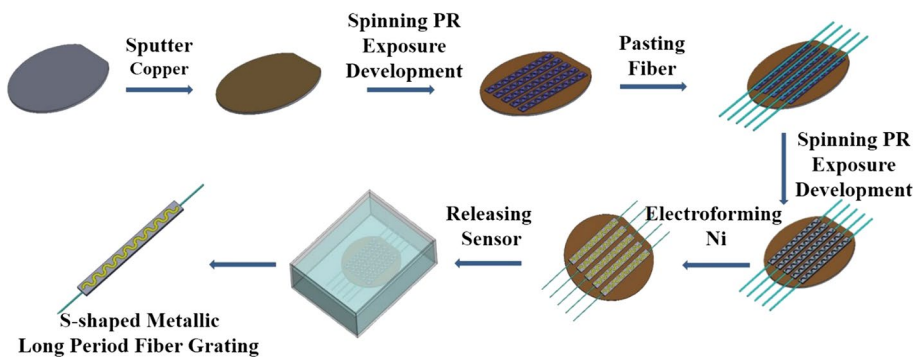
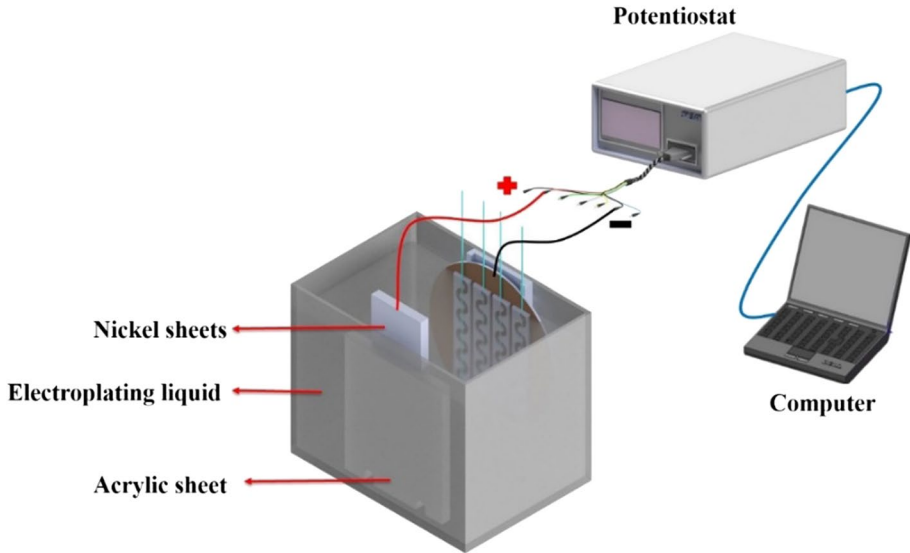


Fig. 1 The S-shaped metallic LPFG fabrication process



**Fig. 2** Schematics of the S-shaped metallic LPFG sensor electroforming process

with buffered oxide etch (BOE) solution before the process was started. First, spin coater processing was performed to evenly spin-coat photoresist onto the surface of the wafer. Second, a double-sided mask aligner was used to produce an exposure pattern mask with a 365-nm wavelength UV light. Then the wafer was immersed in a developing solution and rotated by a spinner to remove areas that were not exposed to the UV light. Upon completion of this operation, the designed bottom periodic structure was obtained. Finally, the etched optical fibre (42  $\mu\text{m}$ ) was pasted onto the patterned SU-8 structure. These procedures were then repeated to form a structure with a thickness of nearly 125  $\mu\text{m}$  to cover the etched optical fibre. Next, the SMLPFG performed the micro-electroforming process described in Sect. 3.2. Last of all, the completed fibre grating on the wafer was immersed in a ferric chloride solution for the releasing process, whereby the photoresist layer was separated from the wafer because the thin copper film sacrificial layer was etched away by the ferric chloride solution.

### 3.2 Electroforming process

The S-shaped MLPFG magnetic field sensor was fabricated using the electroforming process. The electroplating solution consisted of a nickel sulfamate bath, and the copper layer of the wafer was used as a conductive layer. The nickel plating bath had the advantages of uniformity, better flatness, low stress, and a fast deposition rate. The wafer completed with the MEMS process was fastened onto the conducting plate so the copper layer on the wafer could conduct with the conducting plate. The electroforming liquid contained a fixed weight of nickel sulfonate, nickel chloride, boric acid, and deionized water and was placed in a glass vessel and stirred for 4 h with a magnetic stirrer. The main source of nickel ions in the electroforming liquid was the nickel sulfamate. The nickel sulfamate concentration influences the plating surface's flatness and charring of the coating, while the nickel

chloride can increase the conductivity of the plating bath and promote the anode dissolution and coating uniformity of the nickel plate. The pH value of the electroforming liquid had to be maintained at 3.7–4.2. Electroforming is an electrochemical reaction that was used to dissolve the anodic metal in the bath and drive the metal ions to be freely deposited onto the cathode pre-plating. After the electroforming liquid was prepared, the wafer and the nickel plate were fixed on the acrylic plate in parallel in the electroforming liquid. As a result, the metal ions released by the anode could effectively fill the photoresist structure region on the wafer. The power used for the electroforming consisted of a potentiostat with a current values were setting to 0.1, 0.3 and 0.2 A, respectively. After the pre-treatment was completed, the temperature of the electroforming liquid was raised to 40 °C, and the current value of the electric chemistry analyser and electroforming time were set to reach the desired thickness (about 130  $\mu\text{m}$ ). The entire wafer was then immersed into the mixed solution of hydrogen peroxide, ammonium water, and deionized water until the copper layer (sacrificial layer) had completely disappeared, which, in turn, allowed the S-shaped MLPFG magnetic field sensor to be released. Figure 3 shows a optical microscope image of the resulting S-shaped MLPFG magnetic field sensor.

### 3.3 The S-shaped MLPFG magnetic field sensing experiment setup

During the process of the magnetic field sensing experiment, we use the S-shaped MLPFG sensor to detect the strength of the external applied magnetic field. To avoid thermal effect, we employ the NdFeB magnet to generate the magnetic field and a gaussmeter to measure the magnetic field. The strength of the magnetic field is determined by adjusting the vertical distance between the NFeB magnet and metallic grating structure of S-shaped MLPFG. The magnetic field attracts the metallic grating structure and induces the variation of strain induced refractive index. The change of transmission loss and wavelength shift were discussed. Figure 4 shows the experimental setup. The purpose of the S-shaped MLPFG magnetic field calibration test was to analyse the changes in optical characteristics when the S-shaped MLPFG was affected by a magnetic field. First, the S-shaped MLPFG sensor's two ends were fastened onto the precision stage and load cell. The magnetic field was controlled by adjusting the vertical distance between the NFeB magnet and metallic grating structure of the S-shaped MLPFG. The magnetic field was increased from 0 Gauss to 350

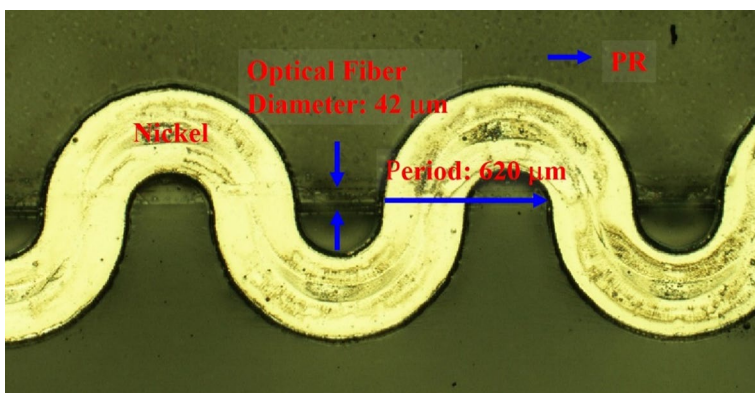
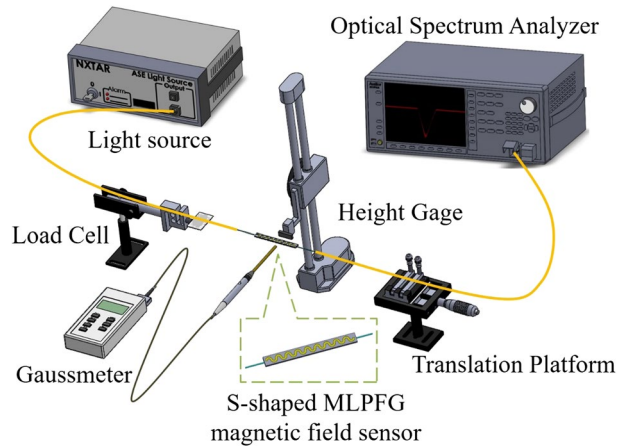


**Fig. 3** A optical microscope image of the of the S-shaped metallic LPPG sensor

**Fig. 4** Experimental setup for S-shaped MLPFG magnetic field sensing experiment



Gauss. The OSA is used to monitor the optical spectra and the S-shaped MLPFG spectra change under the magnetic field being analysed.

## 4 Results and discussion

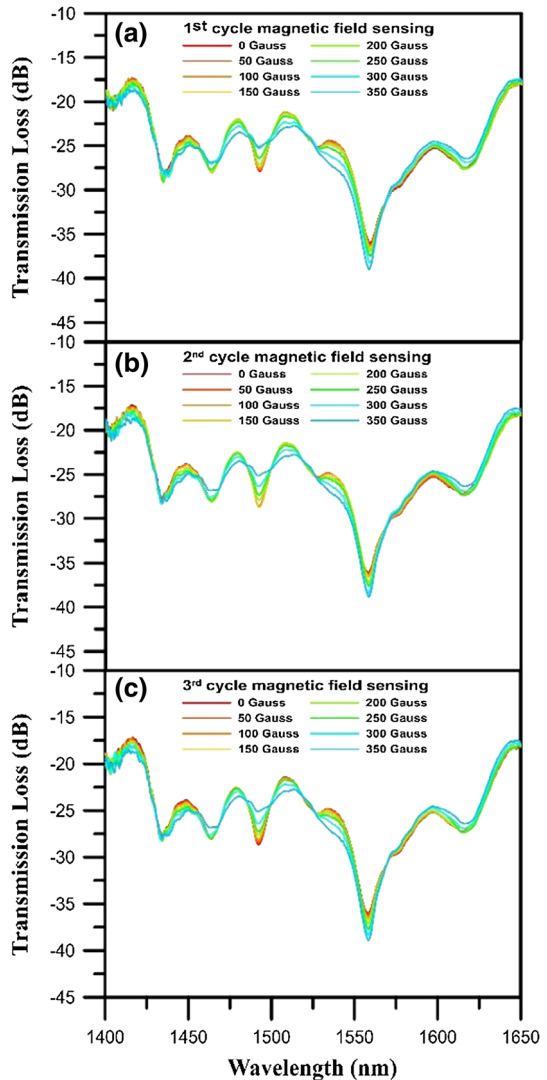
### 4.1 S-shaped MLPFG magnetic field sensor

In this study, a novel LIGA-like process involving lithography and electroforming was used to develop an MLPFG with a periodic S-shaped polymer-metal structure. By applying the LIGA process, the SU-8 3050 photoresists could be sandwiched to enclose the single mode fibre (SMF) to form a periodic S-shaped photoresist structure, after which the nickel could be electroformed to fill up the S-shaped photoresist grating area, which was itself composed of a combination of the photoresist and nickel. The period of the resulting MLPFG was 620  $\mu\text{m}$ , the total grating length was 2.5 cm, and the radius of the optical fibre was 21  $\mu\text{m}$ .

### 4.2 S-shaped MLPFG magnetic field sensing experiment

The results of the S-shaped MLPFG magnetic field sensing experiment showed that, when unaffected by magnetic force, the resonant wavelength of the sensors was 1558.591 nm and the transmission loss was  $-35.995$  dB, and that the resonant wavelength slightly changed while the transmission loss gradually decreased as the intensity of the magnetic field applied was increased. At a magnetic field of 350 Gauss, the resonant wavelength was 1558.342 nm, and the transmission loss was  $-39.024$  dB. The transmission loss increased gradually, dropping by 3.029 dB as shown in Fig. 5a. Figure 6a is a wavelength-transmission loss analysis chart for the S-shaped MLPFG magnetic field sensing test. The figure shows the resonant wavelength positions and transmission loss changes from 0 to 350 Gauss. As the magnetic field increased, the transmission loss changes and the magnetic field shared a linear relationship, with a transmission loss sensitivity of  $-0.0083$  dB/Gauss and a linearity ( $R^2$ ) of 0.911.

**Fig. 5** First through third cycle S-shaped MLPGF spectra of magnetic field sensing

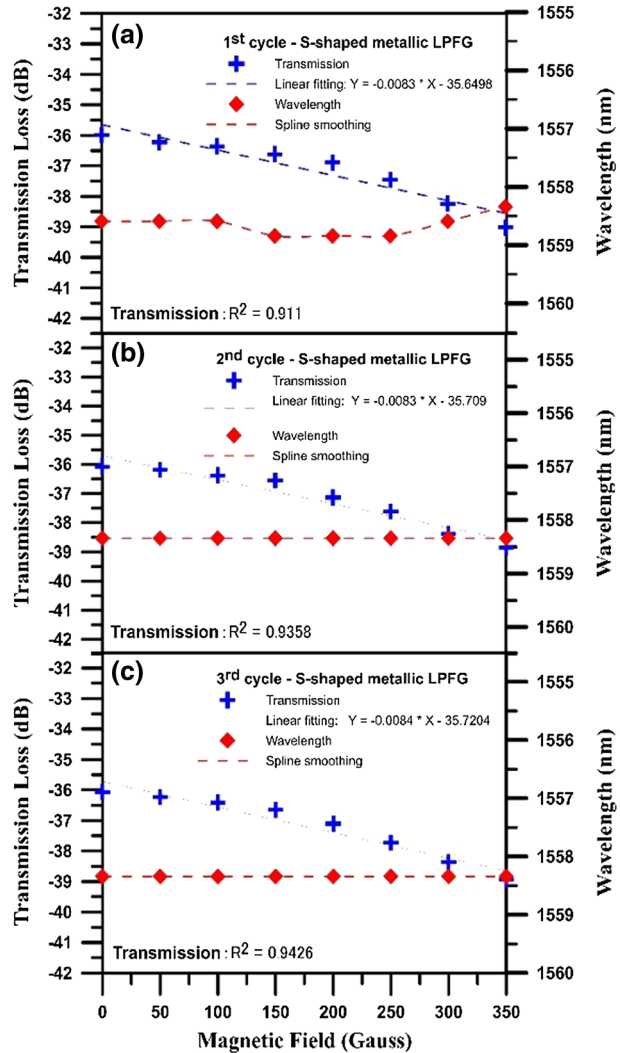


### 4.3 Magnetic field sensing cyclic test

To explore the repeatability of the S-shaped MLPGF magnetic field sensors, the procedures used in the first experiment were repeated for two more magnetic sensing experiments. The results of the second experiment showed that when unaffected by a magnetic force, the resonant wavelength was 1558.342 nm and the transmission loss was  $-36.082$  dB, and that the resonant wavelength was unchanged while the transmission loss gradually decreased as the intensity of the magnetic field applied was increased. At a magnetic field of 350 Gauss, the resonant wavelength was 1558.324 nm, and the transmission loss was  $-38.855$  dB. Transmission loss increased gradually, dropping by 2.773 dB as shown in Fig. 5b. Figure 6b is a wavelength-transmission loss analysis chart for the second S-shaped MLPGF magnetic field sensing test. The figure shows that as the magnetic flux increased,

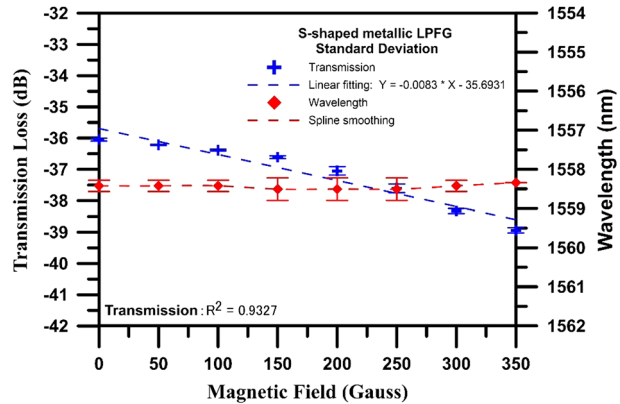


**Fig. 6** First through third magnetic field sensing correction graphs for wavelength- magnetic field -transmission



the transmission loss changes and the magnetic field shared a linear relationship, with a transmission loss sensitivity of  $-0.0083$  dB/Gauss and a linearity ( $R^2$ ) of 0.9358. The results of the third experiment showed that when unaffected by magnetic force, the resonant wavelength was at 1558.342 nm and transmission loss was  $-36.066$  dB, and that the resonant wavelength was unchanged while the transmission loss gradually decreased as the intensity of the magnetic field applied was increased. At a magnetic field of 350 Gauss, the resonant wavelength was 1558.342 nm, and the transmission loss was  $-38.945$  dB. The transmission loss increased gradually, dropping by 2.879 dB as shown in Fig. 5c. Figure 6c is a wavelength-transmission analysis chart for the third S-shaped MLPFG magnetic field sensing test. The figure shows that as the magnetic field increased, the transmission loss changes and the magnetic field shared a linear relationship, with a transmission loss sensitivity of  $-0.0084$  dB/Gauss and a linearity ( $R^2$ ) of 0.9426. The three magnetic field sensing experiments revealed that when the magnetic field was modulated, the change in the

**Fig. 7** Standard deviation analysis results for the S-shaped MLPFG magnetic field sensing over the three cycles



transmission loss had good reproducibility and stability as shown in Fig. 7. The standard deviations for sensitivity and linearity ( $R^2$ ) from the three experiments were  $-0.0083$  dB/Gauss and  $0.9327$ , respectively. The sensitivity to transmission loss in this study was  $6.64$  times greater than the sensitivity of  $0.00125$  dB/Gauss reported by Konstantaki et al. (2011). The results suggest that this phenomenon was caused by the magnetic nickel metal. The external magnetic field attracts the nickel structure and strains the periodic metal grating structure, which leads to perturbations in the metal grating's periodic refractive index.

## 5 Conclusion

The S-shaped MLPFG magnetic field sensor developed in this study used photolithography and electroforming to produce an S-shaped metallic periodic structure. The fibre etching and photoresist process parameters affected the long-period structure of the sensor. During the electroforming process, the ionic liquid concentration, current density, and processing time affected the pore size of the sensor, and the uniformity of electroforming thickness affected the quality of the sensor. The magnetic field intensity was increased from  $0$  Gauss to  $350$  Gauss; the highest sensitivity of the magnetic field sensor was  $-0.0084$  dB/Gauss and  $R^2$  was  $0.9426$ . The sensitivity to transmission loss of the magnetic field sensor developed in this study was  $6.64$  times better than that proposed by Konstantaki et al. (2011). The cyclic magnetic field treatment experimental results showed that the S-shaped MLPFG has excellent repeatability. Therefore, the S-shaped MLPFG sensor developed in this study can be used to measure magnetic field intensity.

**Acknowledgement** This work was supported by the Ministry of Science and Technology, Taiwan (Grant Number 107-2623-E-992-301-D).

## References

- Allsop, T., Arif, R., Neal, R., Kalli, K., Kundrát, V., Rozhin, A., Culverhouse, P., Webb, D.J.: Photonic gas sensors exploiting directly the optical properties of hybrid carbon nanotube localized surface plasmon structures. *Light Sci. Appl.* **5**(2), 1–8 (2016)
- Bandara, A.B., Zuo, Z., Ramachandran, S., Ritter, A., Hefflin, J.R., Inzana, T.J.: Detection of methicillin-resistant staphylococci by biosensor assay consisting of nanoscale films on optical fiber long-period gratings. *Biosens. Bioelectron.* **70**, 433–440 (2015)

- Berruti, G., Consales, M., Borriello, A., Giordano, M., Buontempo, S., Breglio, G., Makovec, A., Petagna, P., Cusano, A.: High-sensitivity metal oxides-coated long-period fiber grating sensors for humidity monitoring in high-energy physics applications. In: *Optical Sensing and Detection III*. International Society for Optics and Photonics, vol. 9141, pp. 914114 (2014)
- Del Villar, I., Fuentes, O., Chiavaioli, F., Corres, J.M., Matias, I.R.: Optimized strain long-period fiber grating (LPG) sensors operating at the dispersion turning point. *J. Lightwave Technol.* **36**(11), 2240–2247 (2018)
- Erdogan, T.: Fiber grating spectra. *J. Lightwave Technol.* **15**, 1277–1294 (1997)
- Gao, L., Zhu, T., Deng, M., Chiang, K.S., Sun, X., Dong, X., et al.: Long-period fiber grating within D-shaped fiber using magnetic fluid for magnetic-field detection. *IEEE Photonics J.* **4**, 2095–2104 (2012)
- Gouveia, C.A.J., Coelho, L., Franco, M.A.R.: Proceedings of SPIE 10323, 25th International Conference on Optical Fiber Sensors (OFS-25), 103233P (2017)
- Jiao, S.X., Zhao, Y., Gu, J.J.: Simultaneous measurement of humidity and temperature using a polyvinyl alcohol tapered fiber bragg grating. *Instrum. Sci. Technol.* **46**, 1–12 (2017)
- Konstantaki, M., Candiani, A., Pissadakis, S.: Optical fibre long period grating spectral actuators utilizing ferrofluids as outclading overlayers. *J. Eur. Opt. Soc. Rapid Publ.* **6**, 11007 (2011)
- Lin, C.Y., Wang, L.A., Chern, G.W.: Corrugated long-period fiber gratings as strain, torsion, and bending sensors. *J. Lightwave Technol.* **19**, 1159–1168 (2001)
- Liu, T., Chen, X., Di, Z., Zhang, J., Li, X., Chen, J.: Tunable magneto-optical wavelength filter of long-period fiber grating with magnetic fluids. *Appl. Phys. Lett.* **91**, 121116 (2007)
- Liu, T., Chen, Y., Han, Q., Lü, X.: Magnetic field sensor based on U-bent single-mode fiber and magnetic fluid. *IEEE Photonics J.* **6**(6), 1–7 (2014)
- Lv, R.Q., Wang, Q., Hu, H.F., Li, J.: Fabrication and sensing characterization of thermally induced long period fiber gratings in few mode fibers. *Optik-Int. J. Light Electron Opt.* **158**, 71–77 (2018)
- Miao, Y., Zhang, K., Liu, B., Lin, W., Zhang, H., Lu, Y., et al.: Ferrofluid-infiltrated microstructured optical fiber long-period grating. *IEEE Photonics Technol. Lett.* **25**, 306–309 (2013)
- Miao, Y., Ma, X., Lin, J., Song, B., Lin, W., Zhang, H., et al.: Intensity-based magnetic field measurement employing tilted long-period fiber gratings. *J. Opt.* **17**, 1–5 (2015)
- Mishra, S.K., Zou, B., Chiang, K.S.: Wide-range pH sensor based on a smart-hydrogel-coated long-period fiber grating. *IEEE J. Sel. Top. Quantum Electron.* **23**, 284–288 (2017)
- Mizuno, Y., Hayashi, N., Fukuda, H., Song, K.Y., Nakamura, K.: Ultrahigh-speed distributed Brillouin reflectometry. *Light Sci. Appl.* **5**, e16184 (2016)
- Najari, M., Javan, A.M., Amiri, N.: Hybrid all-fiber sensor for simultaneous strain and temperature measurements based on mach-zehnder interferometer. *Optik-Int. J. Light Electron Opt.* **126**(19), 2022–2025 (2015)
- Shew, B.Y., Kuo, C.H., Huang, Y.C., Tsai, Y.H.: UV-LIGA interferometer biosensor based on the SU-8 optical waveguide. *Sens. Actuators A* **120**, 383–389 (2005)
- Singh, A., Engles, D., Sharma, A., Singh, M.: Temperature sensitivity of long period fiber grating in SMF-28 fiber. *Optik-Int. J. Light Electron Opt.* **125**(1), 457–460 (2014)
- Tan, Y.C., Ji, W.B., Mamidala, V., Chow, K.K., Tjin, S.C.: Carbon-nanotube-deposited long period fiber grating for continuous refractive index sensor applications. *Sens. Actuators B Chem.* **196**, 260–264 (2014)
- Thomas, S., Mathew, J., Radhakrishnan, P., Nampoory, V.P.N., George, A.K., Al-Harhi, S.H., Ramanujan, R.V., Anantharaman, M.R.: Metglas thin film based magnetostrictive transducers for use in long period fibre grating sensors. *Sens. Actuators A* **161**(1), 83–90 (2010a)
- Thomas, S., Mathew, J., Radhakrishnan, P., Nampoory, V., George, A., Al-Harhi, S.: Metglas thin film based magnetostrictive transducers for use in long period fibre grating sensors. *Sens. Actuators A* **161**, 83–90 (2010b)
- Yang, M., Dai, J., Zhou, C., Jiang, D.: Optical fiber magnetic field sensors with TbDyFe magnetostrictive thin films as sensing materials. *Opt. Express* **17**(23), 20777–20782 (2009)
- Yin, M.J., Huang, B., Gao, S., Zhang, A.P., Ye, X.: Optical fiber LPG biosensor integrated microfluidic chip for ultrasensitive glucose detection. *Biomed. Opt. Express* **7**(5), 2067–2077 (2016)
- Zhang, N.M.Y., Dong, X., Shum, P.P., Hu, D.J.J., Su, H., Lew, W.S., et al.: Magnetic field sensor based on magnetic-fluid-coated long-period fiber grating. *J. Opt.* **17**, 065402 (2015)
- Zhao, Y., Lei, M., Liu, S.X., Zhao, Q.: Smart hydrogel-based optical fiber SPR sensor for pH measurements. *Sens. Actuators B Chem.* **261**, 226–232 (2018)
- Zheng, J., Dong, X., Zu, P., Shao, L.-Y., Chan, C.C., Cui, Y., Shum, P.P.: Magnetic field sensor using tilted fiber grating interacting with magnetic fluid. *Opt. Express* **21**(15), 17863–17868 (2013)
- Zheng, Z.M., Yu, Y.S., Zhang, X.Y., Guo, Q., Sun, H.B.: Femtosecond laser inscribed small-period long-period fiber gratings with dual-parameter sensing. *IEEE Sens. J.* **18**, 1100–1103 (2018)